

GRB090111: extra soft steep decay emission and peculiar re-brightening

R. Margutti^{1,2*}, T. Sakamoto³, G. Chincarini^{1,2}, C. Guidorzi^{4,2}, J. Mao^{2,6}, F. Pasotti²,
D. Burrows⁵, P. D’Avanzo¹, S. Campana², S.D. Barthelmy³, N. Gehrels³

¹ *Università degli studi Milano Bicocca, P.za della Scienza 3, Milano 20126, Italy*

² *INAF Osservatorio Astronomico di Brera, via Bianchi 46, Merate 23807, Italy*

³ *NASA/Goddard Space Flight Center, Greenbelt, MD 20771, USA*

⁴ *Dipartimento di Fisica, Università di Ferrara, via Saragat 1, I-44100, Ferrara, Italy*

⁵ *Department of Astronomy and Astrophysics, Pennsylvania State University, 525 Davey Lab, University Park, PA 16802, USA*

⁶ *Yunnan Observatory, Chinese Academy of Sciences, Kunming, Yunnan Province, China*

Accepted 200? Month Day Received 2009 Month Day; in original form 2009 March 19

ABSTRACT

We present a detailed study of GRB 090111, focusing on its extra soft power-law photon index $\Gamma > 5$ at the very steep decay phase emission (power-law index $\alpha = 5.1$, steeper than 96% of GRBs detected by *Swift*) and the following peculiar X-ray re-brightening. Our spectral analysis supports the hypothesis of a comoving Band spectrum with the the peak of the νF_ν spectrum evolving with time to lower values: a period of higher temporal variability in the 1-2 keV light-curve ends when the E_{peak} evolves outside the energy band. The X-ray re-brightening shows extreme temporal properties when compared to a homogeneous sample of 82 early flares detected by *Swift*. While an internal origin cannot be excluded, we show these properties to be consistent with the energy injection in refreshed shocks produced by slow shells colliding with the fastest ones from behind, well after the internal shocks that are believed to give rise to the prompt emission have ceased.

Key words: gamma-ray: bursts – radiation mechanism: non-thermal – X-rays: individual (GRB090111).

1 INTRODUCTION

The unprecedented fast re-pointing capability of *Swift* (Gehrels et al. 2004) has ushered in a new era in the study of Gamma Ray Bursts (GRB) sources. A canonical picture of the X-ray afterglow light-curve emerged (see e.g. Nousek et al. 2006), with five different components describing the overall structure observed in the majority of events: an initial steep decay, a shallow-decay plateau phase, a normal decay, a jet-like decay component as well as randomly occurring flares.

The steep decay phase smoothly connects to the prompt emission (e.g. Tagliaferri et al. 2005), with a typical temporal power law decay index between 2 and 4 (Evans et al. 2009a): this strongly suggests a common physical origin. The observed spectral softening with time challenges the simplest version of the most popular theoretical model for this phase, the High Latitude Emission (HLE) model

(Fenimore et al. 1996; Kumar & Panaitescu 2000): according to this scenario, steep decay photons originate from the delayed prompt emission from different viewing latitudes of the emitting area (Zhang, Liang & Zhang 2007) and are expected to lie on a simple power law (SPL) spectral model. The 0.3 – 10 keV spectrum of the steep decay phase is generally consistent with the expected SPL behaviour with a typical photon index $\Gamma \sim 2$ (see Evans et al. 2009a); however, a careful inspection of the GRBs with the best statistics reveals that alternative explanations are required (see e.g. Zhang et al. 2009; Qin et al. 2009). Deviations from the SPL spectral model are therefore of particular interest.

Flares have been found to be a common feature of early X-ray afterglows: with a typical duration over occurrence time $\Delta t/t \sim 0.1$ (Chincarini et al. 2007) and a Band spectrum (Band et al. 1993) reminiscent of the typical spectral shape of the prompt emission (Falcone et al. 2007), they are currently believed to be related to the late time activity by the central engine. In spite of the growing statistics their origin is still an open issue.

In this paper we analyse and discuss how and if the

* E-mail: raffaella.margutti@brera.inaf.it (RM)

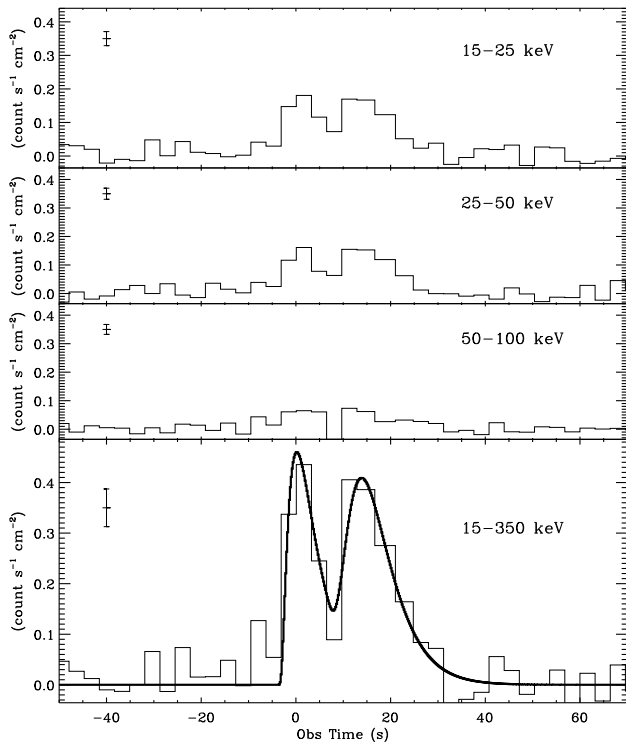


Figure 1. BAT mask weighted light-curve in different energy bands (binning time of 3.2 s). No signal is detected above 100 keV. Bottom panel, solid black line: 15 – 350 keV light-curve best fit. The typical 1σ error size is also shown in each panel.

extra soft ($\Gamma > 5$) steep decay emission of GRB090111 fits into different theoretical models; particular attention will be devoted to the possible link with the detected soft prompt 15 – 150 keV emission. After the steep decay, the GRB090111 0.3 – 10 keV light-curve shows a peculiar re-brightening, with extreme properties when compared to typical X-ray flares: alternative explanations are discussed. The paper is organised as follows: observations are described in Sect. 2; the details of the data analysis are reported in Sect. 3. Our results are discussed in Sect. 4. Conclusions are drawn in Sect. 5. Uncertainties and upper limits are quoted at the 90% confidence level (c.l.) unless otherwise stated.

2 SWIFT OBSERVATIONS

The Swift Burst Alert Telescope (BAT; Barthelmy et al. 2005) triggered and located GRB090111 at 23:58:21 UT on 2009-01-11. The spacecraft immediately slewed to the burst allowing the X-ray Telescope (XRT; Burrows et al. 2005) and the UV/Optical Telescope (UVOT, Roming et al. 2005) to collect data starting 76.6 s and 86 s after the trigger, respectively. A refined position was quickly available: R.A.(J2000)= $16^{\text{h}}46^{\text{m}}42.14^{\text{s}}$, Dec.(J2000)= $+00^{\circ}04'38.2''$ with a 90% error radius of 1.7 arcsec (Evans et al. 2009b). No source was detected by the UVOT at the X-ray afterglow position (Hoversten & Sakamoto 2009). No prompt ground based ob-

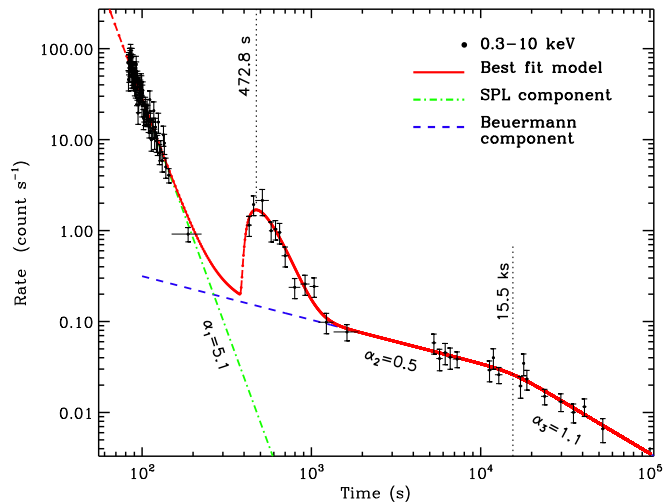


Figure 2. XRT 0.3 – 10 keV light-curve with best fit superimposed.

servation was reported, probably due to the vicinity (46°) to the Sun.

The data were processed with the HEASOFT v. 6.6.1 package and corresponding calibration files: standard filtering and screening criteria were applied. BAT data analysis was based on the event data recorded from -240 s to 960 s. XRT data were acquired in Windowed Timing (WT) mode until around 150 s; after that time the XRT automatically switched to the Photon Counting (PC) mode to follow the decaying source photon flux. Between $\sim 150 \sim 690$ s PC data were affected by pile-up: in this time interval an annular region of events extraction with the exclusion radius estimated following the prescriptions of Moretti et al. (2005) was used instead of a circular region. The resulting 0.3 – 10 keV light-curve is shown in Fig. 2: the chosen data binning assures a minimum signal to noise ratio (SNR) equal to 4; when single orbit data were not able to fulfil this requirement, data coming from different orbits were merged to build a unique data point.

3 ANALYSIS AND RESULTS

The BAT light curve (Fig. 1) shows a double-peaked structure with $T_{90}(15 - 350 \text{ keV}) = 24.8 \pm 2.7 \text{ s}$ (Stamatikos et al. 2009). It can be fit using two Norris et al. (2005) profiles peaking at $t_{\text{peak},1} = 4.2 \pm 1.2 \text{ s}$ and $t_{\text{peak},2} = 9.3 \pm 1.1 \text{ s}$; the two structures are characterised by a $1/e$ rise and decay times $t_{\text{rise},1} = 2.6 \pm 0.5 \text{ s}$, $t_{\text{decay},1} = 6.6 \pm 0.5 \text{ s}$, $t_{\text{rise},2} = 4.5 \pm 0.4 \text{ s}$, $t_{\text{decay},2} = 8.8 \pm 1.3 \text{ s}$ and a width $w_1 = 9.1 \pm 1.0 \text{ s}$ and $w_2 = 13.3 \pm 1.6 \text{ s}$. The amplitude is $A_1 = 0.46 \pm 0.13 \text{ (count s}^{-1} \text{ cm}^{-2})$ and $A_2 = 0.38 \pm 0.04 \text{ (count s}^{-1} \text{ cm}^{-2})$. The parameters are defined following Norris et al. (2005), while their uncertainty is computed accounting for their covariance and quoted at 68% c.l.

The time averaged BAT spectrum can be fit by a soft single power-law photon index $\Gamma = 2.37 \pm 0.18$ with a total fluence $S(15 - 150 \text{ keV}) = (6.2 \pm 1.1) \times 10^{-7} \text{ erg cm}^{-2}$ ($\chi^2/\text{dof} = 55.92/56$). The fluence ratio $S(25 - 50 \text{ keV})/S(50 - 100 \text{ keV}) = 1.29 \pm 0.20$ (68% c.l.) places GRB090111 at the boundary between X-Ray Rich (XRR)

and X-Ray Flash (XRF) events according to the classification of Sakamoto et al. (2008). The BAT data alone are not able to constrain the E_p parameter (peak energy of the νF_ν spectrum): however, fixing the low energy photon index α_B of a Band model at -1 (typical value for both GRBs and XRFs, see e.g. Sakamoto et al. 2005) we derive $E_p < 32$ keV. Using the $E_p - \Gamma$ relation developed by Sakamoto et al. (2009) we have $E_p < 27$ keV, in agreement with the previous result.

The X-ray light-curve (Fig.2) exhibits a steep decay which is best fit by a simple power law with index $\alpha_1 = 5.1 \pm 0.2$ ($\alpha_1 = 4.6 \pm 0.2$) and $T_0 = 0$ s ($T_0 = 9.3$ s, peak time of the second prompt pulse). This is followed by a re-brightening which dominates the light-curve between 420 and 900s. During this time period no detection can be reported in the 15-150 keV energy range. After the re-brightening the light curve flattens to a simple power law index $\alpha_2 = 0.5 \pm 0.2$, while starting from 15 ks the count rate decays as $\alpha_3 = 1.1 \pm 0.3$ (Fig. 2). The re-brightening can be fit adding a Norris et al. (2005) component with amplitude $A = 1.53 \pm 0.23$ counts s^{-1} , start time $t_s = 370$ s ($\chi^2/\text{dof} = 84.8/93$) and rise and decay times $t_{\text{rise}} = 69.3 \pm 8.9$ s $t_{\text{decay}} = 212.3 \pm 37.5$ s; a width $w = 281.6 \pm 39.2$ s; a peak time $t_{\text{peak}} = 472.8 \pm 21.0$ and an asymmetry parameter $k = 0.51 \pm 0.04$ of Norris et al. (2005). This implies a T_{90} of ~ 675 s. In this time interval, the light-curve experiences a re-brightening to underlying continuum fluence ratio $S_{\text{reb}}/S_{\text{cont}} \sim 4.7$, while the relative flux variability is $\Delta F/F = 14.2 \pm 2.1$ (where ΔF is the re-brightening contribution to the total flux at t_{peak} and F is underlying power-law flux at the same time). All uncertainties related to the light-curve fitting are quoted at 68% c.l.

The steep decay spectrum ($77\text{s} < t < 150\text{s}$) can be modelled using an absorbed simple power-law with photon index $\Gamma = 5.1 \pm 0.4$ and neutral hydrogen column density $N_{\text{H},0} = (4.9 \pm 0.8) \times 10^{21} \text{ cm}^{-2}$ in excess of the Galactic value in this direction which is $6.5 \times 10^{20} \text{ cm}^{-2}$, (Kalberla et al. 2005) ($\chi^2/\text{dof} = 68.77/49$). While a pure black body emission model is ruled out, the addition of a black body component statistically improves the fit: however, the data are not able to simultaneously constrain the black body temperature and intrinsic absorption so that only rough 2σ limits can be quoted: $0.2 \text{ keV} < kT_b < 0.8 \text{ keV}$, ($0.5 < N_{\text{H},0} < 5$) $\times 10^{22} \text{ cm}^{-2}$. The X-ray data can alternatively be fit by simultaneously modelling the Galactic and host absorption at the proper redshift. We find two sets of allowed parameters: the first is for a close GRB with $N_{\text{H},z} = (0.63^{+0.14}_{-0.09}) \times 10^{22} \text{ cm}^{-2}$, $z = 0.5^{+0.2}_{-0.3}$ and $\Gamma = 4.4 \pm 0.2$ ($\chi^2/\text{dof} = 40.5/49$, Pval = 80%). The second solution is for a distant and heavily absorbed GRB: $N_{\text{H},z} = (8.8^{+2.8}_{-6.1}) \times 10^{22} \text{ cm}^{-2}$, $z = 3.8^{+0.2}_{-0.3}$ and $\Gamma = 4.0 \pm 0.2$ ($\chi^2/\text{dof} = 48.6/49$, Pval = 49%). The fit is not able to constrain the redshift parameter: however the detection of $N_{\text{H},z}$ in excess of the Galactic value (at $z = 0$) suggests $z < 1.8$ according to the Grupe et al. (2007) relation.

Spectral evolution is apparent from Fig. 3, with the $(1-2) \text{ keV}/(0.3-1) \text{ keV}$ hardness ratio starting to decrease 100s after the trigger: it is interesting to note that this corresponds to the end of a period of higher temporal variability detected in the $1-2 \text{ keV}$ light-curve. This kind of variability is not seen in the $0.3-1 \text{ keV}$ data. A comparison of the light-curves extracted in the two energy bands reveals a depletion

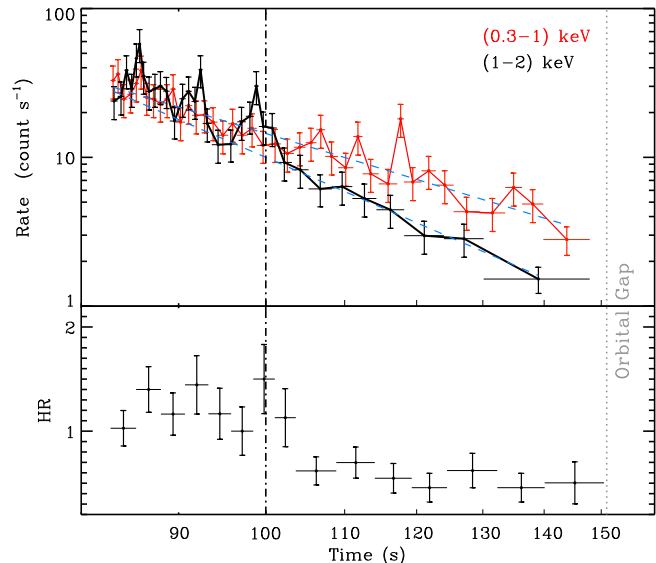


Figure 3. Upper panel: red (black) points: 0.3–1 keV (1–2 keV) XRT light-curve rebinned at constant signal to noise ratio SNR = 4. Blue dashed lines: best fit simple power law models. Lower panel: hardness ratio $\text{HR} = (1-10) \text{ keV}/(0.3-1) \text{ keV}$ evolution with time. The dashed-dotted vertical line marks the beginning of the HR decrease.

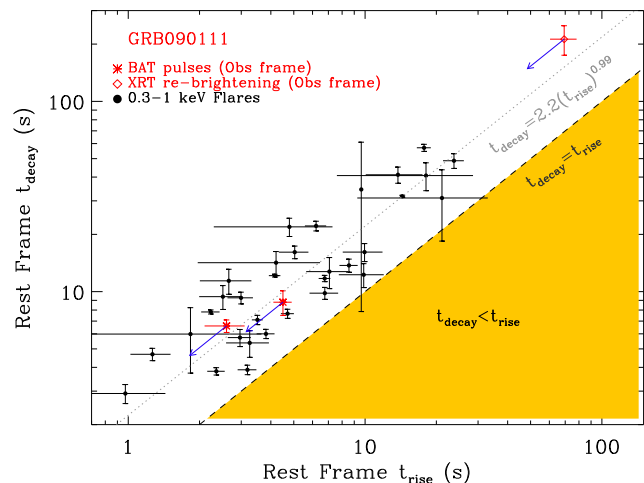


Figure 4. Decay time versus rise time for a sub-sample of 32 early time flares identified in the 0.3-10 keV energy range in GRBs with red-shift (Chincarini et al.2009 in prep.) and for GRB090111. The blue arrows track the shift of the data when the red-shift correction is applied. The black dashed line corresponds to the $t_{\text{decay}} = t_{\text{rise}}$ locus, while the best fit power-law model is indicated with a grey dotted line: $t_{\text{decay}} = (2.2 \pm 0.1) t_{\text{rise}}^{(0.99 \pm 0.02)}$ (1σ c.l.).

of high energy photons with time: while the $0.3-1 \text{ keV}$ best fit simple power-law decay index is $\alpha_1 = 4.3 \pm 0.3$, the continuum higher energy ($1-2 \text{ keV}$) photon flux decay is steeper, being modelled by $\alpha_2 = 5.6 \pm 0.5$.

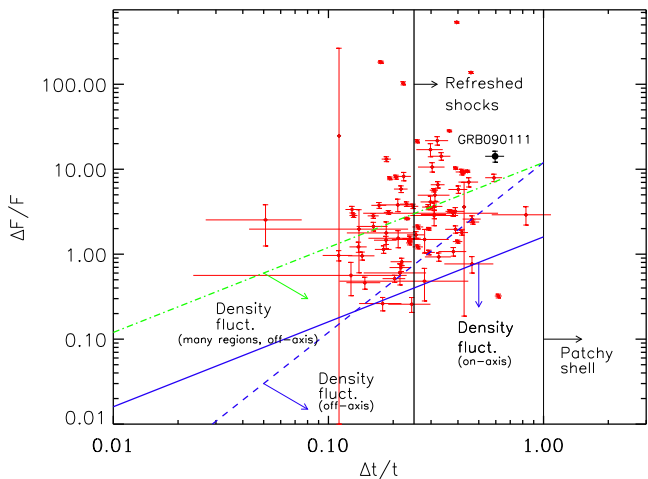


Figure 5. Relative variability flux ($\Delta F/F$) kinematically allowed regions as a function of relative variability time scale $\Delta t/t$ for a sample of 81 early ($t_{\text{peak,obs}} < 1000$ s) flares identified in 54 different GRBs (Chincarini et al. 2009 in prep.). The three limits shown have been computed according to Eq. 7 and A2 of Ioka et al. 2005. The position of GRB090111 is marked with a filled black dot.

4 DISCUSSION

4.1 Unusual spectral properties

GRB 090111 shows a very steep ($\alpha = 5.1 \pm 0.2$, 68% c.l.) and soft decay (spectral index $\beta = 4.1 \pm 0.4$): out of 295 GRB X-ray light-curves showing the canonical steep-shallow-normal decay transition analysed by Evans et al. (2009a), only 11 (4%) events are characterised by an initial power law index steeper than the one observed in GRB 090111. Such a high value suggests that this is the beginning of the tail of a flare whose onset was missed by the XRT. The spectral analysis leads to the same conclusion: out of 1242 time resolved XRT spectra of *Swift*-GRB in the time period April 2005 - September 2008, we found the existence of very soft absorbed simple power-law photon indices $\Gamma > 5$ in GRB050714B, GRB050822 and GRB060512: in each of these cases, the soft spectral emission is linked to flare activity in the XRT light-curve. (The three bursts also show a soft BAT prompt emission, with a time averaged 15-150 keV photon index $\Gamma \sim 2.4 - 2.5$). If this is the case, the comoving spectrum is likely to be a Band spectrum whose E_{peak} evolves to lower values.

Both the BAT prompt photon index steeper than 2, and the XRT photon index $\Gamma > 4$ steeper than the typical Band low-energy photon index $\alpha_B \sim -1$ (see e.g. Kaneko et al. 2006, Sakamoto et al. 2005) suggest that in both cases the observed emission is dominated by the beta portion of the comoving Band spectrum. It is interesting to note that fixing $\alpha_B \sim -1$ in the prompt spectrum we obtain $28 \text{ keV} < E_{\text{peak}} < 30 \text{ keV}$ at 3σ level for a high energy photon index $-5 < \beta_B < -4$ which matches the unusual value of the high energy photons index measured in XRT. This establishes a spectral connection between the XRT steep decay and the prompt emission, provided that the E_{peak} had shifted well inside the XRT energy range by the beginning of the observation as found in other GRBs

and XRFs (e.g. GRB060614, Mangano et al. 2007a; XRF 050416A, Mangano et al. 2007b). At the same time the very soft emission observed extends the distribution in β_B to very low values: only $\sim 10\%$ of the spectra of 156 BATSE GRBs either have $\beta_B < -4$ or do not have any high energy component (see e.g. Kaneko et al. 2006).

During the steep decay spectral evolution is apparent (Fig. 3, lower panel). We split the steep decay phase into two time intervals, taking 100 s as dividing line as suggested by the hardness ratio evolution. A simultaneous fit of the two spectra with an absorbed cut-off power-law model (with E_{peak} as a free parameter of the fit) shows that for each ($N_{\text{H,z}}, z$) there exists a statistically acceptable solution with $E_{\text{peak},1} = 1.0^{+0.2}_{-0.1}$ keV and $E_{\text{peak},2} < 0.3$ keV, where the subscripts 1 and 2 refer to the first ($t < 100$ s) and second ($t > 100$ s) time interval, respectively. This suggests that the detected spectral evolution can be linked to the evolution of the E_{peak} to lower values. It is worth noting that the higher temporal variability characterising the 1-2 keV signal in the first 100 s (Fig. 3) disappears as the peak energy evolves outside the energy band.

4.2 Peculiar re-brightening: a flare?

Interpreting the X-ray re-brightening as onset of the afterglow, it is possible to infer the initial Lorentz factor Γ_0 of the fireball from the light-curve peak time (see Molinari et al. 2007 and references therein). For a homogeneous surrounding medium with particle density $n_0 = 1 \text{ cm}^{-3}$, radiative efficiency $\eta = 0.2$ we have $\Gamma_0 \sim 180(1+z)^{3/8}(E_\gamma/10^{53} \text{ erg})^{1/8}$. From $z < 1.8$ we derive an intrinsic peak energy $E_{\text{p,i}} < 84 \text{ keV}$ and isotropic energy $E_{\text{iso}} < 9 \times 10^{51} \text{ erg}$ (well within the 2σ region of the Amati 2006 relation). This translates into a conservative upper limit $\Gamma_0 < 100$: this is lower than what is commonly found for normal GRBs ($\Gamma_0 \sim 500$, see e.g. Molinari et al. 2007), and consistent with the less-Lorentz-boosted interpretation of XRRs and XRFs (see Zhang 2007 for a review). A similar result has been found for other XRFs: see e.g. XRF080330 (Guidorzi et al. 2009).

In the context of off-axis emission, it is worth noting that the X-ray re-brightening experienced by GRB090111 is a sharp feature, reaching a flux contrast $\Delta F/F \sim 14$ during a rising time of only ~ 70 s. Granot (2005) showed that both on-axis and off-axis decelerating jets can only produce smooth bumps in the afterglow emission. We therefore consider this hypothesis unlikely.

A much more likely explanation is suggested by Fig. 4 where the temporal properties of the GRB090111 BAT pulses and of the XRT re-brightening are shown to be consistent with the best fit relation found for the intrinsic properties of 32 0.3-10 keV early time flares (Chincarini et al. 2009, in prep.). This fact, together with the consistency with the typical $t_{\text{rise}}/t_{\text{decay}} \sim 0.3 - 0.5$ (Norris et al. 1996) found for prompt pulses, would suggest a common internal shock origin.

Alternatively the bump could be due to refreshed shocks (Rees & Meszaros 1998). Following the calculations of Ioka, Kobayashi & Zhang (2005) we plot in Fig. 5 the $\Delta F/F$ and $\Delta t/t$ values for the X-ray bump of GRB090111 together with the values coming from a homogeneous analysis of 82 early ($t_{\text{peak}} < 1000$ s) flares identified in 54 different GRBs by Chincarini et al. 2009

in prep.: all the flares (including the GRB090111 bump) were fit using the same Norris et al. (2005) profile, defining the width of each pulse as the time interval between the $1/e$ intensity points. Figure 5 shows the kinematically allowed regions for bumps produced by density fluctuations (Wang & Loeb 2000; Lazzati et al. 2002; Dai & Lu 2002) seen on-axis, off-axis and by many regions according to eq. 7 and A2 in Ioka, Kobayashi & Zhang (2005); bumps due to patchy shells (Meszaros, Rees & Wijers 1998; Kumar & Piran 2000) occupy the $\Delta t > t$ region, while refreshed shocks account for the $\Delta t > t/4$ area. From this figure it is apparent that the X-ray bump of GRB090111 lies in the refreshed shocks region: density fluctuations are ruled out.

5 CONCLUSIONS

GRB090111 shows an extra soft $\Gamma > 5$ steep decay emission. This is likely due to an intrinsic Band spectrum whose low energy power law is missed because of the limited energy range of the XRT. The peak energy of the spectrum evolves through the XRT band producing a softening trend testified by the different light-curve decay behaviours in different energy bands. It's interesting to note that the period of higher temporal variability in the 1-2 keV light-curve ends when the E_{peak} shifts outside the energy band. The steep decay is followed by an X-ray re-brightening whose peculiar temporal properties made it worth a detailed study. While the temporal properties of the re-brightening are consistent with an internal origin, with $\Delta t/t \sim 0.6$ and $\Delta F/F \sim 14$ the bump lies in the refreshed shocks region of Fig. 5. Density fluctuations are ruled out. Finally, with a fluence ratio $S(25 - 50 \text{ keV})/S(50 - 100 \text{ keV}) = 1.29 \pm 0.20$ (68% c.l.) we propose this event to be classified as XRR090111.

ACKNOWLEDGEMENTS

We thank the referee for constructive criticism. This work is supported by ASI grant SWIFT I/011/07/0, by the Ministry of University and Research of Italy (PRIN MIUR 2007TNYZXL), by MAE and by the University of Milano Bicocca (Italy).

REFERENCES

- Amati, L. 2006, MNRAS, 372, 233
 Band, D. Matteson, J. Ford, L. et al. 1993, ApJ, 413, 281
 Barthelmy, S. D. Barbier, L. M. Cummings, J. R. et al. 2005, SSRv, 120, 143
 Burrows, D. N. Hill, J. E. Nousek, J. A. et al. 2005, SSRv, 120, 165
 Chincarini, G. Moretti, A. Romano, P. et al. 2007, ApJ, 671, 1903
 Dai, Z. G. & Lu, T. 2002, ApJ, 565, L87
 Evans, P. A. Beardmore, A. P. Page, K. L. et al. 2009a, MNRAS accepted
 Evans, P. A. Goad, M. R. Osborne, J. P. et al. 2009b, GCN Circ. 8796
 Falcone, A. D. Morris, D. Racusin, J. et al. 2007, ApJ, 671, 1921
 Fenimore, E. E. Madras, C. D. Nayakshin, S. 1996, ApJ, 473, 998
 Gehrels, N. Chincarini, G. Giommi, P. et al. 2004, ApJ, 611, 1005
 Granot, J. 2005, ApJ, 631, 1022
 Grupe, D. Nousek, J. A. vanden Berk, D. E. et al. 2007, AJ, 133, 2216
 Guidorzi, C. Clemens, C. Kobayashi, S. et al. 2009, A&A, 499, 439
 Hoversten, E. A. & Sakamoto, T. 2009, GCN Circ. 8799
 Ioka, K. Kobayashi, S. & Zhang, B. 2005, ApJ, 631, 429
 Kalberla, P. M. W. Burton, W. B. Hartmann, D. et al. 2005, A&A, 440, 775
 Kaneko, Y. Preece, R. D. Briggs, M. S. et al. 2006, ApJS, 166, 298
 Kumar, P. & Panaitescu, A. 2000, ApJ, 541, L51
 Kumar, P. & Piran, T. 2000, ApJ, 535, 152
 Lazzati, D. Rossi, E. Covino, S. et al. 2002, A&A, 396, L5
 Mangano, V., Holland, S. T., Malesani, D. et al., 2007a, A&A, 470, 105
 Mangano, V., La Parola, V., Cusumano et al., 2007b, ApJ, 654, 403
 Meszaros, P. Rees, M. J. & Wijers, R. A. M. J. ApJ, 1998, 499, 301
 Molinari, E. Vergani, S. D. Malesani, D. et al. 2007, A&A, 469, 13
 Moretti, A. Campana, S. Mineo, T. et al. 2005, SPIE, 5898, 360
 Norris, J. P. Bonnell, J. T. Kazanas, D. et al. 2005, ApJ, 627, 324
 Norris, J. P. Nemiroff, R. J. Bonnell, J. T. et al. 1996, ApJ, 459, 393
 Nousek, J. A. Kouveliotou, C. Grupe, D. et al. 2006, ApJ, 642, 389
 Qin, Y.-P. 2009, ApJ, 691, 811
 Rees, M. J. & Meszaros, P. 1998, ApJ, 496, L1
 Roming, P. W. A. Kennedy, T. E. Mason, K. O. et al. SSRv, 120, 95
 Sakamoto, T. Lamb, D. Q. Kawai, N. et al. 2005, ApJ, 629, 311
 Sakamoto, T. Hullinger, D. Sato, G. et al. 2008, ApJ, 679, 570
 Sakamoto, T. Sato, G. Barbier, L. et al. 2009, ApJ, 693, 922
 Savaglio, S. Glazebrook, K. & LeBorgne, D. 2009, ApJ, 691, 182
 Schlegel, D. J. Finkbeiner, D. P. & Davis, M. 1998, ApJ, 500, 525
 Stamatikos, M. Barthelmy, S. D. Baumgartner, W. H. et al. 2009, GCN Circ. 8800
 Tagliaferri, G. Goad, M. Chincarini, G. et al. 2005, Nature, 436, 985
 Wang, X. & Loeb, A. 2000, ApJ, 535, 788
 Zhang, B. B. Liang, E. W. Zhang, B. 2007, ApJ, 666, 1002
 Zhang, B. 2007, ChJAA, 7, 1
 Zhang, B.-B. , Zhang, B. , Liang, E.-W. et al. 2009, ApJ, 690, L10

This paper has been typeset from a \TeX / \LaTeX file prepared by the author.